CHARACTERIZATION OF TURBULENT TRANSITION AND SHOCK/BOUNDARY-LAYER INTERACTION IN SHOCK TUBES

Yong Sun*[a)], Matthias Ihme*, and Ralf Deiterding[†]
*Department of Aerospace Engineering, University of Michigan, Ann Arbor, 48105, USA
[†] Computer Science and Mathematics Division, Oak Ridge National Laboratory, Oak Ridge, TN 37831, USA

MOTIVATION

Shock tube systems are invaluable in providing detailed information about ignition delay times, extinction limits and species time-histories for the development and validation of reaction mechanisms. Although the flow-field in shock-tubes can be reasonably described using idealized gas-dynamic theory, practical systems exhibit considerable sources of non-idealities that result from the development of viscous boundary layers, shock-attenuation, and shock-bifurcation. The direct consequences of these non-idealities are increasing uncertainties in measurements and associated errors of derived rate coefficients and ignition delay times.

The objective of this work is to conduct detailed simulations in shock-tubes at practically relevant operating conditions in order to quantify direct contributions of the boundary layer development on the incident shock wave attenuation and to investigate the development of the reflected shock-wave interaction.

NUMERICAL APPROACH

The flow-field in a shock-tube is a multi-scale problem, containing a highly localized shock-structure, a laminar or turbulent boundary, and – in the case of an ignition study – also chemical reactions and species conversion. To accurately resolves this wide range of scales, the AMR-framework AMROC (Adaptive Mesh Refinement in Object-Oriented C++) is utilized [1]. AMROC employs a block-structured adaptive mesh refinement (AMR) method [2], in which individual regions in the flow-domain are successively refined subject to a specific refinement criterion. These refined blocks are derived recursively from the coarser level so that a hierarchy of successively embedded grid patches is constructed.

To accurately describe the turbulence and shock-structure inside the shock-tube, a hybrid discretization scheme is employed. This scheme combines a Weighted Essentially Non-Oscillatory (WENO) scheme with a central difference (CD) scheme for describing the smooth flow-field away from the shock [4]. The WENO scheme uses a bandwidth-optimization techniques to develop symmetric optimal stencils in order to minimize the dissipation and improve resolution efficiency. The WENO/CD hybrid scheme relies on a switching criterion to distinguish regions of smooth flow (using CD) and regions that contain strong gradients and shock-discontinuities. Liu's entropy condition and gradients of pressure and density are hereby used to formulate this switch [4]. To reduce computational cost and to describe the shock-tube geometry in its natural geometry, the governing equations were implemented in a cylindrical coordinate system in AMROC. A third-order strong stability preserving Runge-Kutta (SSPRK) scheme is used for time advancement.

RESULTS

Boundary Layer Development Behind Incident Shock

To validate the implementation of the cylindrical coordinate formulation in AMROC, a grid-convergence study is performed, and results are compared against analytical results from compressible laminar boundary-layer theory [5]. In this configuration, the fluid in the driver and driven sections are air at a pressure of 0.02 bar and 0.18 bar, respectively. The temperature in the driven section is 290 K. Results of this grid-convergence study are presented in Fig. 1(a). Five different refinement levels are considered, and it can be seen that the predicted boundary layer converges to the theoretical results [5].

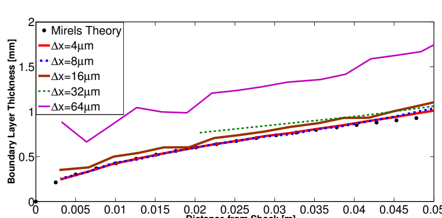

(a) Convergence plot comparing numerically predicted boundary layer thickness against theoretical results [5]

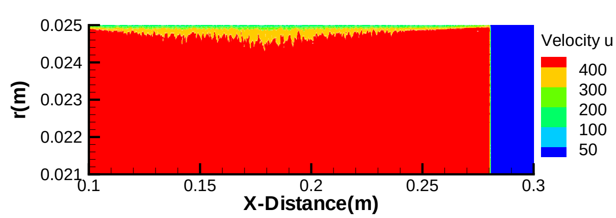

(b) Boundary-layer transition

Figure 1. Boundary-layer development behind incident shock-wave.

To investigate the laminar/turbulent transition mechanism behind an incident shock, nitrogen is considered as gas and

[a)] Corresponding author. E-mail: yosun@umich.edu

the pressure in the driven and driver sections were respectively 1.8 bar and 16 bar. The initial temperature in the driven section is 490K. An instantaneous flow-field result, showing the axial velocity field, is presented in Fig. 1(b). A laminar boundary layer is initially formed behind the incident shock, and subsequently transitions to a turbulent regime.

Interaction of Boundary Layer with Reflected Shock

The results presented in Fig. 2 show the shock bifurcation after the shock is reflected at the end wall and propagates backward where it interacts with the boundary layer. Under the operating conditions investigated, the shock bifurcation is clearly evident. Due to the differences in stagnation pressures across the shock, the boundary layer cannot pass smoothly into the reflected shock region. Therefore, the boundary layer lifts off, resulting in the formation of a separation region. The flow eventually stagnates and reverses direction, leading to the formation of a viscous layer at the wall under the bifurcated shock. Due to the entropy difference between the flow traveling through the bifurcation and the flow which encounters the normal shock, a slip shear layer is formed, and the slip line is unstable and eventually rolls up to form discrete vortices.

The instantaneous temperature and pressure along the centerline and three different time-instances are shown in Fig. 3. Both the pressure and temperature at the end wall reach the value predicted by a one-dimensional inviscid theory. The overshoot can be seen as the result of reattachemetn shock in the rear of of the interaction zone, which is similar to those in steady-state shock-wave/boundary-layer interactions serving to turn the flow parallel to the wall. It can be anticipated that these variation in pressure and temperature can affect the ignition in shock tube systems, leading to potential errors in ignition delay times.

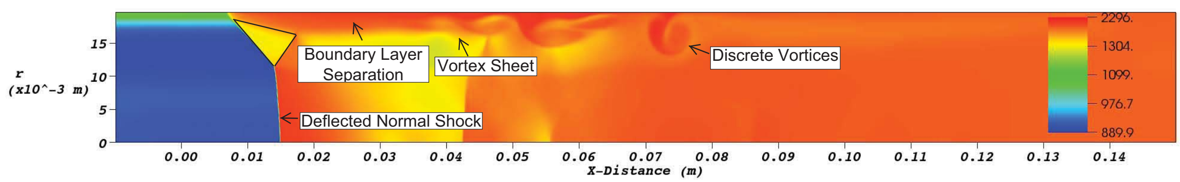

Figure 2. Shock Bifurcation showing shock/boundary layer interaction: Temperature Contour

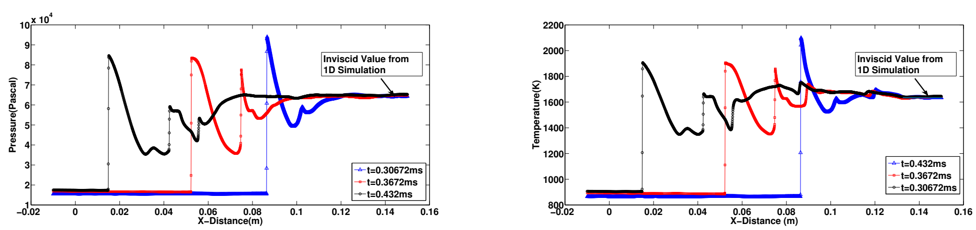

(a) pressure at the centerline

(b) temperature at the centerline

Figure 3. Instantaneous variation for various times in the simulation

CONCLUSION

An adaptive mesh-refinement technique in combination with high-order WENO/CD scheme is extended to cylindrical coordinate system to model shock/boundary layer interaction and shock-bifurcation in shock-tubes. The results of the laminar boundary layer development are consistent with Mirels' compressible boundary layer theory. The transition of the boundary layer is captured and the transitional Reynolds number agrees with experimental data. Shock bifurcation is clearly observed in the simulation and a physical explanation is provided for the structure and instantaneous temperature and pressure variation.

References

[1] Deiterding R. *AMROC - Blockstructured Adaptive Mesh Refinement in Object-oriented C++*, available at web site amroc.sourceforge.net.

[2] Berger, M. J. and Colella, P.: J. Comp. Phys. *Local adaptive mesh refinement for shock hydrodynamics*, **82**:64–84, 1989.

[3] Parashar, M., and Browne, J. C.:In Proc. 29th Hawaii Int. Conf. on System Sciences. *On partitioning dynamic adaptive grid hierarchies*, Jan. 1996.

[4] Ziegler J. L., Deiterding R., Shepherd J.E., Pullin D.I.: J. Comp. Phys. *An adaptive high-order hybrid scheme for compressive, viscous flows with detailed chemistry*, **230**:7598–7630, 2011.

[5] Mirels, H.: Phys. Fluids. *Correlation formulas for laminar shock tube boundary layer*, **9**(**7**):1265–1272, 1966.

[6] Dillon E. Jr.: In AIAA 20th Aerospace Sciences. *Heat Transfer Rate for Laminar, Transition and Turbulent Boundary Layer and Transition Phenomenon on Shock Tube Wall: Numerical Analysis Using Finite Element Method*, Jan. 11-14, 1982.

[7] Petersen E. L., Hanson R. K.: Shock Waves. *Nonideal effects behind reflected shock waves in a high-pressure shock tube*, **10**:405–420, 2001.

[8] Bowman C. T., Hanson R. K.: J. Phys. Chem. *Shock Tube Measurements of Rate Coefficients of Elementary Gas Reactions*, **83**:757, 1979.